American Journal of Applied Mathematics
2026; 14(4): 244-258
http://www.sciencepublishinggroup.com/j/ajam
doi: 10.11648/j.ajam.20261404.17

Memory-Driven Anisotropic Expansion in Bianchi Type-IV Space-Time via Nonlocal Fractional Operators

Anil Kumar Menaria*

Department of Mathematics and Statistics, Bhupal Nobles' University, Udaipur, India

Email address:
menaria.anilkumar@gmail.com (Anil Kumar Menaria)

To cite this article:
Anil Kumar Menaria. (2026). Memory-Driven Anisotropic Expansion in Bianchi Type-IV Space-Time via Nonlocal Fractional Operators. *American Journal of Applied Mathematics, 14*(4), 244-258. https://doi.org/10.11648/j.ajam.20261404.17

Received: 1 July 2026; **Accepted:** 11 July 2026 **Published:** 14 August 2026

Abstract: Anisotropic cosmological models play an important role in describing the evolution of the early universe, where directional expansion and spatial curvature cannot be neglected. Classical Bianchi models, however, are formulated through local differential equations and therefore do not account for hereditary effects that may influence the interaction between geometry and matter over cosmic time scales. Motivated by the growing use of nonlocal fractional operators in mathematical physics, this work develops a memory-dependent Bianchi type–IV cosmological model by incorporating the Atangana–Baleanu–Caputo fractional derivative into the reduced Einstein evolution equations. The resulting formulation preserves the characteristic curvature contribution through the explicit A^{-2} geometric potential and leads to a closed nonlinear dynamical system governing the directional scale factors and directional Hubble parameters. The analytical study is carried out by transforming the fractional model into an equivalent Volterra integral equation, from which existence and uniqueness of solutions are established using Banach's fixed-point theorem. Additional theoretical results provide admissibility conditions for the energy density together with a sufficient criterion for the asymptotic decay of anisotropy under suitable expansion assumptions. To investigate the influence of nonlocal memory, a predictor–corrector numerical scheme is implemented for several fractional orders. The computational results demonstrate that decreasing the fractional order strengthens hereditary effects, slows the decay of the shear scalar and anisotropy parameter, delays isotropization, and produces a measurable memory lag in the expansion dynamics while recovering the classical Einstein evolution as the fractional order approaches unity. These findings show that the proposed framework offers a mathematically consistent and computationally reproducible extension of Bianchi type–IV cosmology, providing a useful approach for investigating memory-driven anisotropic evolution within the setting of fractional gravitational dynamics.

Keywords: Bianchi Type-IV, Atangana-Baleanu Derivative, Nonlocal Memory, Anisotropic Cosmology, Existence and Uniqueness, Isotropization

1. Introduction

Spatial homogeneity is one of the most productive simplifications in mathematical cosmology, yet homogeneity does not force isotropy. Bianchi space–times provide the canonical setting in which the Universe expands uniformly in space while allowing different directional expansion rates. Such anisotropic models have long served as a theoretical laboratory: they permit the study of anisotropy decay, shear evolution, and the sensitivity of cosmological dynamics to initial conditions [1–3]. In addition, anisotropic cosmologies provide useful approximations to the early Universe where high-energy processes may naturally generate shear, viscosity, or directional stresses.

The Bianchi classification enumerates all three-dimensional real Lie algebras that act simply transitively on spatial hypersurfaces [4–6]. While Bianchi types I, V, and IX dominate the applied literature due to their relatively direct connection with flat/open/closed Friedmann–Lemaître–Robertson–Walker (FLRW) limits, Bianchi type–IV is less explored despite its richer algebraic structure and capacity for more intricate anisotropic behaviours. This motivates a careful investigation of type–IV dynamics with modern modelling ingredients.

A central modelling direction in contemporary applied mathematics is the systematic introduction of memory. Standard cosmological equations are local in time: the dynamics at time t depends only on present values. However, a variety of effective descriptions of complex systems exhibit hereditary effects, where past evolution influences the current response. Nonlocal time operators provide a mathematical framework for incorporating such memory, and fractional calculus has become a natural tool to represent these effects.

Among nonlocal operators, the Atangana–Baleanu fractional derivative in Caputo sense (ABC derivative) is particularly attractive. Its kernel is non-singular and expressed through the Mittag–Leffler function, interpolating between exponential-like and power-law-like memory decay[7, 8]. This makes ABC derivatives suitable for modelling systems where memory fades in a physically realistic manner without singularities at the origin. Motivated by these features, we introduce ABC operators into the anisotropic expansion of Bianchi type–IV space–time and investigate the resulting memory-driven dynamics.

Novelty and contributions. Although fractional derivatives have been employed in various Bianchi-type cosmologies, the present work differs in several essential aspects. First, we focus on the Bianchi type–IV geometry and retain its characteristic curvature potential explicitly through the exponential-type potential terms proportional to A^{-2}, rather than absorbing curvature into implicit source functions. Second, this analytical curvature representation yields a closed anisotropic dynamical system that is directly verifiable and reproducible. Third, by rewriting the ABC-fractional field equations in an equivalent Volterra integral form, we establish well-posedness via fixed-point arguments in a manner that is intrinsically tied to the fully specified curvature structure. Finally, the proposed predictor–corrector discretization and parameter disclosure provide a transparent numerical pipeline, enabling consistent reconstruction of shear, anisotropy and acceleration diagnostics across different memory orders α.

2. Mathematical Preliminaries: ABC Operators, Integral Form, and Core Lemmas

This section introduces the fractional tools required for the subsequent analytical development. Throughout, $T > 0$ is fixed and $0 < \alpha < 1$. We denote by $C([0,T])$ the Banach space of continuous functions on $[0,T]$ equipped with the norm $\|u\|_\infty = \sup_{t\in[0,T]} |u(t)|$.

2.1. Atangana-baleanu Fractional Operators

Definition 2.1 (Atangana–Baleanu–Caputo derivative [9, 10]). Let $f \in C^1([0,T])$ and $0 < \alpha < 1$. The Atangana–Baleanu derivative in the Caputo sense (ABC derivative) is

$$ {}^{ABC}D_t^\alpha f(t) = \frac{B(\alpha)}{1-\alpha}\int_0^t f'(\tau)\, E_\alpha\left(-\frac{\alpha}{1-\alpha}(t-\tau)^\alpha\right) d\tau, \quad (1)$$

where $B(\alpha)$ is a normalization function satisfying $B(0) = B(1) = 1$.

Definition 2.2 (Atangana–Baleanu fractional integral). For $f \in L^1(0,T)$ and $0 < \alpha < 1$, define the AB fractional integral as

$$\begin{aligned} {}^{AB}I_t^\alpha f(t) &= \frac{1-\alpha}{B(\alpha)} f(t) \\ &+ \frac{\alpha}{B(\alpha)\Gamma(\alpha)}\int_0^t (t-\tau)^{\alpha-1} f(\tau) d\tau. \end{aligned} \quad (2)$$

2.2. Integral Reformulation

The ABC derivative is naturally handled via an equivalent integral equation. This converts the fractional differential problem into a Volterra-type problem suited for fixed-point arguments.

Lemma 2.1 (ABC integral representation). Let $f \in C([0,T])$ and consider the initial value problem

$$ {}^{ABC}D_t^\alpha u(t) = f(t),\ u(0) = u_0.$$

Then u satisfies the integral equation

$$\begin{aligned} u(t) &= u_0 + \frac{1-\alpha}{B(\alpha)} f(t) \\ &+ \frac{\alpha}{B(\alpha)\Gamma(\alpha)}\int_0^t (t-\tau)^{\alpha-1} f(\tau) d\tau. \end{aligned} \quad (3)$$

Conversely, any continuous solution of the above equation satisfies the ABC differential equation.

2.3. Basic Inequalities and Functional Estimates

The following estimates will be used repeatedly.

Lemma 2.2 (AB kernel bound). For $0 < \alpha < 1$ and $t \in [0,T]$,

$$\int_0^t (t-\tau)^{\alpha-1} d\tau = \frac{t^\alpha}{\alpha} \le \frac{T^\alpha}{\alpha}.$$

Lemma 2.3 (Lipschitz integral estimate). Let $g : [0,T]\times\mathbb{R}^m \to \mathbb{R}^m$ be Lipschitz in the second argument with constant $L > 0$:

$$\|g(t,x) - g(t,y)\| \le L\|x-y\|.$$

Then for any $X, Y \in C([0,T];\mathbb{R}^m)$ and each $t \in [0,T]$,

$$\begin{aligned} &\left\|\int_0^t (t-\tau)^{\alpha-1}\ \big(g(\tau,X(\tau)) - g(\tau,Y(\tau))\big)d\tau\right\| \\ &\qquad \le \frac{T^\alpha}{\alpha} L\|X-Y\|_\infty. \end{aligned}$$

2.4. ABC–Mittag–Leffler Stability Lemma [11, 12]

For qualitative analysis we require a decay estimate compatible with ABC memory.

Lemma 2.4 (ABC relaxation bound). Let $y \in C([0,\infty))$ satisfy

$$^{ABC}D_t^{\alpha} y(t) \le -\lambda y(t), \;\; y(0) = y_0, \quad \lambda > 0.$$

Then

$$0 \le y(t) \le y_0\, E_\alpha(-\kappa t^\alpha) \;\; (t \ge 0),$$

for a constant $\kappa > 0$ depending on α, λ, and $B(\alpha)$. In particular, $y(t) \to 0$ as $t \to \infty$.

3. Bianchi Type–IV Space–Time: Geometry and Kinematic Observables

In this section we specify the geometric background and introduce the kinematic quantities used to describe anisotropic expansion. The expressions derived here will be employed both in the analytical part and in the numerical simulations.

3.1. Metric and Spatial Homogeneity

We consider the following spatially homogeneous anisotropic Bianchi type–IV space–time [13–15]:

$$ds^2 = -dt^2 + A(t)^2\, dx^2 + B(t)^2 e^{2x}\, dy^2 + C(t)^2 e^{2x}\, dz^2, \tag{4}$$

where $A(t), B(t), C(t) > 0$ are the directional scale factors. The exponential factor e^{2x} encodes the nontrivial structure constants of the Bianchi type–IV Lie algebra and distinguishes this geometry from the simpler Bianchi type–I setting.

For later use, define the spatial volume scale factor (average scale factor)

$$V(t) = A(t)B(t)C(t), a(t) = V(t)^{1/3} = (A(t)B(t)C(t))^{1/3}.$$

The quantity $a(t)$ reduces to the usual FLRW scale factor when isotropy is recovered.

3.2. Directional Hubble Rates and Expansion Scalar [16]

The classical directional Hubble parameters are

$$H_1(t) = \frac{\dot{A}(t)}{A(t)}, \quad H_2(t) = \frac{\dot{B}(t)}{B(t)}, \quad H_3(t) = \frac{\dot{C}(t)}{C(t)}.$$

The mean Hubble expansion rate is

$$H(t) = \frac{1}{3}\big(H_1(t) + H_2(t) + H_3(t)\big) = \frac{1}{3}\frac{\dot{V}(t)}{V(t)} = \frac{\dot{a}(t)}{a(t)}.$$

The expansion scalar is given by

$$\theta(t) = H_1(t) + H_2(t) + H_3(t) = 3H(t).$$

3.3. Shear Scalar and Anisotropy Parameter [13, 15]

The shear tensor measures directional distortion of the expansion. For homogeneous diagonal models it is customary to work with the shear scalar

$$\begin{aligned} \sigma^2(t) &= \frac{1}{2}\left(\sum_{i=1}^{3} H_i(t)^2 - \frac{1}{3}\theta(t)^2\right) \\ &= \frac{1}{2}\left[H_1^2 + H_2^2 + H_3^2 - \frac{1}{3}(H_1 + H_2 + H_3)^2\right]. \end{aligned} \tag{5}$$

Clearly $\sigma^2 \ge 0$, and $\sigma^2 = 0$ if and only if $H_1 = H_2 = H_3$, i.e., isotropic expansion.

A dimensionless measure of anisotropy is the anisotropy parameter

$$\Delta(t) = \frac{1}{3}\sum_{i=1}^{3}\left(\frac{H_i(t) - H(t)}{H(t)}\right)^2. \tag{6}$$

When $H(t) \ne 0$, we have $\Delta(t) = 0$ exactly in the isotropic case and $\Delta(t) > 0$ otherwise.

Remark 3.1. The quantities σ^2 and Δ are closely related. In particular, one can express

$$\sigma^2(t) = \frac{3}{2} H(t)^2\, \Delta(t),$$

which implies that anisotropy decay can equivalently be investigated through the decay of σ^2 or Δ.

3.4. Deceleration Parameter

For the purpose of interpreting accelerated expansion we introduce the deceleration parameter

$$q(t) = -1 - \frac{\dot{H}(t)}{H(t)^2}, \tag{7}$$

whenever $H(t) \ne 0$. The phase $q(t) < 0$ corresponds to accelerated average expansion.

3.5. Matter Sector: Anisotropic Fluid

To close the cosmological model we consider an anisotropic energy–momentum tensor of the form

$$T^\mu_{\ \nu} = \mathrm{diag}\big(-\rho(t),\, p_x(t),\, p_y(t),\, p_z(t)\big), \tag{8}$$

where $\rho(t)$ denotes the energy density and p_x, p_y, p_z denote directional pressures. For numerical simulations, a common closure is the linear directional equation of state

$$p_x = \omega_x \rho, \;\; p_y = \omega_y \rho, \;\; p_z = \omega_z \rho,$$

where $\omega_x, \omega_y, \omega_z$ are constants (or slowly varying functions). This closure captures anisotropic stress in a controllable parametric manner and is suitable to investigate memory-driven isotropization.

4. Einstein Tensor–Driven Memory Extension in Bianchi Type–IV Space–Time

This section derives the Einstein field equations for the Bianchi type–IV geometry (4) and introduces a memory-driven generalization using the Atangana–Baleanu–Caputo (ABC) fractional derivative. A key feature of the present formulation is that the curvature/structure contributions induced by the exponential factors e^{2x} are kept *explicit*, yielding a completely closed and reproducible dynamical system.

4.1. Classical Einstein Equations for the Metric (4) [13–15]

Consider the Bianchi type–IV space–time equation (4) and define the directional Hubble parameters

$$H_1 = \frac{\dot{A}}{A},\;\; H_2 = \frac{\dot{B}}{B},\;\; H_3 = \frac{\dot{C}}{C},$$

and the expansion scalar and mean Hubble rate

$$\Theta = H_1 + H_2 + H_3,\;\; H = \frac{1}{3}\Theta.$$

We assume an anisotropic fluid source

$$T^{\mu}{}_{\nu} = \mathrm{diag}\big(-\rho,\, p_x,\, p_y,\, p_z\big), \tag{9}$$

where $p_x = \omega_x\rho,\; p_y = \omega_y\rho,\; p_z = \omega_z\rho,\; \rho(t) \geq 0$ and $\omega_x, \omega_y, \omega_z$ are constants.

The Einstein field equations ($c = 1$)

$$G^{\mu}{}_{\nu} = 8\pi\, T^{\mu}{}_{\nu} \tag{10}$$

reduce, for (4), to the diagonal system

$$\begin{aligned} G^0{}_0 &= -\Big(H_1H_2 + H_2H_3 + H_3H_1\Big) + \frac{3}{A^2} \\ &= 8\pi\rho, \end{aligned} \tag{11}$$

$$\begin{aligned} G^1{}_1 &= -\Big(\dot{H}_2 + \dot{H}_3 + H_2^2 + H_3^2 + H_2H_3\Big) + \frac{1}{A^2} \\ &= 8\pi p_x, \end{aligned} \tag{12}$$

$$\begin{aligned} G^2{}_2 &= -\Big(\dot{H}_1 + \dot{H}_3 + H_1^2 + H_3^2 + H_1H_3\Big) + \frac{1}{A^2} \\ &= 8\pi p_y, \end{aligned} \tag{13}$$

$$\begin{aligned} G^3{}_3 &= -\Big(\dot{H}_1 + \dot{H}_2 + H_1^2 + H_2^2 + H_1H_2\Big) + \frac{1}{A^2} \\ &= 8\pi p_z. \end{aligned} \tag{14}$$

All off–diagonal components vanish for (4). The reproducible computation supporting (11)–(14) is provided in Appendix 8.

4.2. Einstein Tensor Decomposition and Curvature Potentials

For conceptual clarity, we rewrite (11)–(14) in the standard decomposition

$$G^0{}_0 = -\Big(H_1H_2 + H_2H_3 + H_3H_1\Big) + \mathcal{U}_0(A, B, C), \tag{15}$$

$$\begin{aligned} G^1{}_1 = &-\Big(\dot{H}_2 + \dot{H}_3 + H_2^2 + H_3^2 + H_2H_3\Big) \\ &+ \mathcal{U}_1(A, B, C), \end{aligned} \tag{16}$$

$$\begin{aligned} G^2{}_2 = &-\Big(\dot{H}_1 + \dot{H}_3 + H_1^2 + H_3^2 + H_1H_3\Big) \\ &+ \mathcal{U}_2(A, B, C), \end{aligned} \tag{17}$$

$$\begin{aligned} G^3{}_3 = &-\Big(\dot{H}_1 + \dot{H}_2 + H_1^2 + H_2^2 + H_1H_2\Big) \\ &+ \mathcal{U}_3(A, B, C). \end{aligned} \tag{18}$$

where the curvature/structure potentials are explicitly

$$\begin{aligned} \mathcal{U}_0(A, B, C) &= \frac{3}{A^2}, \\ \mathcal{U}_1(A, B, C) = \mathcal{U}_2(A, B, C) = \mathcal{U}_3(A, B, C) &= \frac{1}{A^2}. \end{aligned} \tag{19}$$

Thus the Bianchi type–IV structure enters the dynamics as a geometric potential controlled by the x-direction scale factor $A(t)$.

4.3. Closed Classical Dynamical System

To obtain a closed first-order system, we use

$$\dot{A} = H_1A,\;\; \dot{B} = H_2B,\;\; \dot{C} = H_3C. \tag{20}$$

From (12)–(14) we obtain the evolution of the directional Hubble rates.

First, solve (12) for $\dot{H}_2 + \dot{H}_3$, then permute indices cyclically and isolate the three unknowns $\dot{H}_1, \dot{H}_2, \dot{H}_3$. This yields the explicit system

$$\dot{H}_1 = -H_1\Theta + H_2H_3 + \frac{1}{A^2} - 4\pi(\omega_y + \omega_z - \omega_x)\rho, \tag{21}$$

$$\dot{H}_2 = -H_2\Theta + H_1H_3 + \frac{1}{A^2} - 4\pi(\omega_x + \omega_z - \omega_y)\rho, \tag{22}$$

$$\dot{H}_3 = -H_3\Theta + H_1H_2 + \frac{1}{A^2} - 4\pi(\omega_x + \omega_y - \omega_z)\rho, \tag{23}$$

where the density ρ is constrained by (11), i.e.

$$\rho(t) = \frac{1}{8\pi}\left[-\Big(H_1H_2 + H_2H_3 + H_3H_1\Big) + \frac{3}{A^2}\right]. \tag{24}$$

Equations (20) and (21)–(24) define a closed Einstein-tensor-driven Bianchi type–IV dynamical system.

Remark 4.1. A key structural feature of the present Bianchi type–IV model is that the spatial-curvature contributions are retained *explicitly* as $A(t)^{-2}$–dependent terms in the Einstein field equations. Hence the system forms a closed, verifiable evolution problem: all curvature potentials entering the directional Hubble rates, shear scalar, and anisotropy parameter are determined uniquely from the metric, rather than being absorbed into auxiliary source functions. This derived closure is essential for reproducibility and for isolating the curvature–memory interplay in the fractional dynamics.

4.4. ABC Fractionalization and Final Closed Memory-driven System [17]

We now generalize the classical dynamical system by incorporating nonlocal temporal memory using the ABC derivative. The guiding principle is:

1) evolve the dynamical degrees of freedom via nonlocal time response, and
2) retain the Einstein-tensor curvature potentials explicitly so that the model remains genuinely Bianchi type–IV.

Accordingly, for $0 < \alpha \leq 1$ we postulate the memory-driven system

$$\begin{aligned} {}^{ABC}D_t^{\alpha} A &= H_1 A, \\ {}^{ABC}D_t^{\alpha} B &= H_2 B, \\ {}^{ABC}D_t^{\alpha} C &= H_3 C, \end{aligned} \tag{25}$$

$$\begin{aligned} {}^{ABC}D_t^{\alpha} H_1 = -H_1\Theta + H_2H_3 + \frac{1}{A^2} \\ - 4\pi(\omega_y + \omega_z - \omega_x)\rho, \end{aligned} \tag{26}$$

$$\begin{aligned} {}^{ABC}D_t^{\alpha} H_2 = -H_2\Theta + H_1H_3 + \frac{1}{A^2} \\ - 4\pi(\omega_x + \omega_z - \omega_y)\rho, \end{aligned} \tag{27}$$

$$\begin{aligned} {}^{ABC}D_t^{\alpha} H_3 = -H_3\Theta + H_1H_2 + \frac{1}{A^2} \\ - 4\pi(\omega_x + \omega_y - \omega_z)\rho. \end{aligned} \tag{28}$$

where the density is determined algebraically by

$$\rho(t) = \frac{1}{8\pi}\left[-\Big(H_1H_2 + H_2H_3 + H_3H_1\Big) + \frac{3}{A^2}\right]. \tag{29}$$

Remark 4.2. *[Physical meaning and modeling status of fractionalization.]* The replacement of the classical time derivative by the Atangana–Baleanu–Caputo (ABC) derivative in (25)–(29) should be interpreted as an *effective nonlocal closure* rather than a fundamental modification of the covariant Einstein field equations. In particular, the model does not claim that the Einstein tensor acquires fractional order in a generally covariant sense. Instead, after imposing the spatially homogeneous Bianchi type–IV symmetry, the field equations reduce to a deterministic dynamical system for the directional expansion variables $X(t) = (H_x, H_y, H_z, \rho, \omega_x, \omega_y, \omega_z)$ in cosmic time. The ABC operator is then introduced at the level of this reduced evolution system to encode hereditary effects in the matter–geometry interaction, consistent with the phenomenology of non-Markovian relaxation and delayed response in anisotropic media.

Remark 4.3. *[On covariance and the choice of variables.]* Since the fractional operator is applied *after* fixing the comoving cosmic time gauge and reducing the covariant equations to their minisuperspace dynamics, the formulation is best viewed as a nonlocal dynamical model in the time domain, not as a fractional tensor calculus on space–time. In this sense, covariance is not violated within the reduced setting: the symmetry reduction singles out a preferred time coordinate (the proper time of fundamental observers), and the ABC kernel introduces memory with respect to this physically distinguished clock. Moreover, applying the ABC derivative directly to the dynamical variables is natural in a state-space interpretation: it corresponds to replacing the local flow $X'(t) = F(X(t), t)$ by a memory-driven law ${}^{ABC}D_t^{\alpha} X(t) = F(X(t), t)$, where the present acceleration depends on the entire past history with exponentially tempered Mittag–Leffler weights. Such a construction preserves dimensional consistency and reduces to the classical Bianchi evolution in the limit $\alpha \to 1$, providing a controllable interpolation between Markovian and hereditary cosmological dynamics.

Define the state vector

$$X(t) = \big(A, B, C, H_1, H_2, H_3\big)^{\top} \in \mathbb{R}^6. \tag{30}$$

Then (25)–(29) can be written compactly as the fractional initial value problem

$${}^{ABC}D_t^{\alpha} X(t) = \mathbb{F}\big(X(t)\big), \quad X(0) = X_0, \tag{31}$$

where the nonlinear vector field $\mathbb{F}$ is explicit due to (29) and the curvature potentials (19).

5. Main Results: Well-Posedness and Late-Time Anisotropy Control

This section establishes the fundamental analytical properties of the explicit memory-driven Bianchi type–IV model derived in Section 4. The model is a closed 6-dimensional ABC fractional system with an algebraic density constraint, hence the analysis must be conducted in a way that (i) respects the positivity of the directional scale factors, and (ii) yields explicitly verifiable conditions tied to the explicit curvature term A^{-2}.

Throughout this section, fix $T > 0$ and $0 < \alpha \leq 1$. We work on the Banach space $C([0, T]; \mathbb{R}^6)$ equipped with the supremum norm [18]:

$$\|X\|_{\infty} := \sup_{t\in[0,T]} \|X(t)\|_{\mathbb{R}^6}.$$

5.1. State Space and Admissible Region

Let

$$X(t) = (A(t), B(t), C(t), H_1(t), H_2(t), H_3(t))^{\top} \tag{32}$$

denote the state vector. Motivated by physical admissibility, we restrict attention to the region

$$\Omega_6 := \Big\{(A, B, C, H_1, H_2, H_3) \in \mathbb{R}^6 : \\ A \geq A_*,\ B \geq B_*, \\ C \geq C_*,\ |H_i| \leq H_*\Big\}. \tag{33}$$

where $A_*, B_*, C_* > 0$ and $H_* > 0$ are fixed.

The density $\rho(t)$ is not evolved independently but is defined by the algebraic constraint

$$\rho(X) = \frac{1}{8\pi}\left[-(H_1H_2 + H_2H_3 + H_3H_1) + \frac{3}{A^2}\right]. \tag{34}$$

Definition 5.1 (Admissible solution). A function $X \in C([0, T]; \Omega_6)$ is called an admissible solution of the memory-driven Bianchi type–IV system if it satisfies the ABC evolution equations (25)–(28) of Section 4 together with the density constraint (34) for all $t \in [0, T]$.

5.2. Integral Formulation and Fixed-point Operator

Let the memory-driven system be written compactly as

$$^{ABC}D_t^\alpha X(t) = \mathbb{F}(X(t)),\ \ X(0) = X_0 \in \Omega_6, \tag{35}$$

where $\mathbb{F} : \Omega_6 \to \mathbb{R}^6$ is induced by (25)–(28) after substituting $\rho = \rho(X)$ from (34).

By the ABC integral representation (Lemma 2.1), (35) is equivalent to

$$X(t) = X_0 + \frac{1-\alpha}{B(\alpha)}\,\mathbb{F}(X(t)) \\ + \frac{\alpha}{B(\alpha)\Gamma(\alpha)}\int_0^t (t-\tau)^{\alpha-1}\,\mathbb{F}(X(\tau))\,d\tau. \tag{36}$$

Define the operator $\mathcal{T} : C([0, T]; \Omega_6) \to C([0, T]; \mathbb{R}^6)$ by

$$(\mathcal{T}X)(t) := X_0 + \frac{1-\alpha}{B(\alpha)}\,\mathbb{F}(X(t)) \\ + \frac{\alpha}{B(\alpha)\Gamma(\alpha)}\int_0^t (t-\tau)^{\alpha-1}\,\mathbb{F}(X(\tau))\,d\tau. \tag{37}$$

Then admissible solutions are precisely fixed points of $\mathcal{T}$ in $C([0, T]; \Omega_6)$.

5.3. Existence and Uniqueness of Solution

We first show that $\mathbb{F}$ is locally Lipschitz on Ω_6.

Lemma 5.1 (Local Lipschitz property of the explicit Bianchi-IV vector field). Let Ω_6 be defined by (33). Then $\mathbb{F}$ in (35) is locally Lipschitz on Ω_6. In particular, there exists $L_\Omega > 0$ such that for all $X, Y \in \Omega_6$,

$$\|\mathbb{F}(X) - \mathbb{F}(Y)\| \leq L_\Omega\|X - Y\|.$$

Proof. Each component of $\mathbb{F}$ is a polynomial combination of A, B, C, H_1, H_2, H_3 and the curvature term A^{-2}, together with the density functional $\rho(X)$ given by (34). On Ω_6 we have $A \geq A_* > 0$, hence A^{-2} is smooth and bounded, and $\rho(X)$ is smooth as a function of X. Therefore all components of $\mathbb{F}$ are continuously differentiable on Ω_6, and hence locally Lipschitz. A global Lipschitz constant on Ω_6 follows from boundedness of the Jacobian on compact subsets of Ω_6.

Theorem 5.1 (Existence and uniqueness). Let $X_0 \in \Omega_6$ and assume $0 < \alpha \leq 1$. Then there exists $T_0 \in (0, T]$ such that the ABC initial value problem (35) admits a unique admissible solution $X \in C([0, T_0]; \Omega_6)$. Moreover, if the solution remains in Ω_6 on $[0, T]$, then it is unique on $[0, T]$.

Proof. Fix a closed ball $\mathbb{B}_R \subset C([0, T_0]; \mathbb{R}^6)$ centered at X_0 with radius $R > 0$ such that $\mathbb{B}_R \subset C([0, T_0]; \Omega_6)$. By Lemma 5.1, $\mathbb{F}$ is Lipschitz on the compact region traced by $\mathbb{B}_R$; let the constant be L_Ω.

Let $X, Y \in \mathbb{B}_R$. Using (37), Lipschitz continuity and Lemma 2.2, we obtain

$$\|(\mathcal{T}X)(t) - (\mathcal{T}Y)(t)\| \leq \frac{1-\alpha}{B(\alpha)}\|\mathbb{F}(X(t)) - \mathbb{F}(Y(t))\| \\ + \frac{\alpha}{B(\alpha)\Gamma(\alpha)}\int_0^t (t-\tau)^{\alpha-1}\|\mathbb{F}(X(\tau)) - \mathbb{F}(Y(\tau))\|\,d\tau \\ \leq \frac{1-\alpha}{B(\alpha)}L_\Omega\|X(t) - Y(t)\| \\ + \frac{\alpha}{B(\alpha)\Gamma(\alpha)}L_\Omega\int_0^t (t-\tau)^{\alpha-1}\|X(\tau) - Y(\tau)\|\,d\tau.$$

Taking the supremum over $t \in [0, T_0]$ yields

$$\|\mathcal{T}X - \mathcal{T}Y\|_\infty \leq \left(\frac{1-\alpha}{B(\alpha)}L_\Omega + \frac{\alpha}{B(\alpha)\Gamma(\alpha)}\frac{T_0^\alpha}{\alpha}L_\Omega\right)\|X - Y\|_\infty.$$

Choose $T_0 > 0$ so that

$$q := \frac{1-\alpha}{B(\alpha)}L_\Omega + \frac{\alpha}{B(\alpha)\Gamma(\alpha)}\frac{T_0^\alpha}{\alpha}L_\Omega < 1. \tag{38}$$

Then $\mathcal{T}$ is a contraction on $\mathbb{B}_R$. Banach's fixed-point theorem yields a unique fixed point X, which solves (36) and hence (35).

Lemma 5.2 (Continuation criterion). Let $X(t)$ be the unique local solution of (25)–(29) on $[0, T_0)$ obtained in Theorem 5.1. Assume that there exists $M > 0$ such that $\|X(t)\| \leq M$ for all $t \in [0, T_0)$. Then $X(t)$ can be extended as a solution of (25)–(29) to an interval $[0, T_0 + \delta]$ for some $\delta > 0$. Consequently, the maximal existence time $T_{\max}$ is finite only if $\limsup_{t\to T_{\max}^-}\|X(t)\| = +\infty$.

Corollary 5.1 (Continuous dependence on initial data). Under the hypotheses of Theorem 5.1, solutions depend continuously on initial conditions. If $X_0, Y_0 \in \Omega_6$ generate solutions X, Y on $[0, T_0]$, then

$$\|X - Y\|_\infty \leq \frac{1}{1-q}\,\|X_0 - Y_0\|,$$

where q is defined by (38).

5.4. Positivity and Boundedness of the Energy Density

Since ρ is algebraically determined by (34), the admissibility of the cosmology requires

$$\rho(t) \geq 0,\ \ t \in [0, T_0].$$

This can be guaranteed by conditions on the initial data and forward invariance.

Proposition 5.1 (Sufficient condition for nonnegative density). Let $X(t) \in \Omega_6$ be an admissible solution on $[0, T_0]$. If

$$H_1(t)H_2(t) + H_2(t)H_3(t) + H_3(t)H_1(t) \leq \frac{3}{A(t)^2};\ \forall t \in [0, T_0],$$

then $\rho(t) \geq 0$ on $[0, T_0]$.

Proof. The claim follows immediately from (34).

Proposition 5.2 (Uniform density bound on invariant sets). Assume $X(t) \in \Omega_6$ for all $t \in [0, T_0]$. Then the density is uniformly bounded on $[0, T_0]$, and one has

$$|\rho(t)| \leq \frac{1}{8\pi}\left(3H_*^2 + \frac{3}{A_*^2}\right), \ \ t \in [0, T_0].$$

Proof. On Ω_6 we have $|H_i| \leq H_*$ and $A \geq A_*$. Hence

$$\left|H_1H_2 + H_2H_3 + H_3H_1\right| \leq 3H_*^2, \ \ \frac{3}{A^2} \leq \frac{3}{A_*^2}.$$

Substitute into (34).

5.5. Memory-driven Control of Anisotropy: A Verifiable Criterion

We now establish an anisotropy-control result that is directly compatible with the proposed system. Define the directional deviation variables

$$\delta_1 := H_1 - H, \quad \delta_2 := H_2 - H, \quad \delta_3 := H_3 - H,$$
$$H = \frac{1}{3}(H_1 + H_2 + H_3).$$

and the anisotropy energy

$$D(t) := \delta_1(t)^2 + \delta_2(t)^2 + \delta_3(t)^2. \tag{39}$$

Note that $D(t) \geq 0$, and $D(t) = 0$ if and only if $H_1 = H_2 = H_3$ (isotropy).

Theorem 5.2 (Sufficient condition for asymptotic isotropization). Let $X(t)$ be an admissible solution of (35) on $[0, \infty)$ satisfying:

1) (*Persistent average expansion*) there exist constants $t_0 \geq 0$ and $H_{\min} > 0$ such that

$$H(t) \geq H_{\min} \ \ \forall t \geq t_0;$$

2) (*Controlled directional stress*) there exists $\eta \geq 0$ such that:

$$\begin{aligned}|p_x(t) - p_y(t)| &+ |p_y(t) - p_z(t)| \\ &+ |p_z(t) - p_x(t)| \\ &\leq \eta\, \rho(t), \quad \forall\, t \geq t_0.\end{aligned}$$

3) (*Curvature decay*) the curvature potential satisfies $A(t) \to \infty$ as $t \to \infty$.

Then there exist constants $\lambda > 0$ and $C > 0$ such that for all $t \geq t_0$,

$${}^{ABC}D_t^{\alpha} D(t) \leq -\lambda D(t) + C\, A(t)^{-2}. \tag{40}$$

Consequently, $D(t) \to 0$ as $t \to \infty$, and hence

$$H_1(t) - H(t) \to 0, \quad H_2(t) - H(t) \to 0, \quad H_3(t) - H(t) \to 0,$$

which implies $\sigma^2(t) \to 0$ and $\Delta(t) \to 0$.

Proof. Subtract the ABC equations (26)–(28) pairwise to obtain fractional evolution inequalities for $H_1 - H_2$, $H_2 - H_3$, and $H_3 - H_1$. Each difference contains: (i) a linear damping term generated by the persistent expansion assumption 1) through the factor $\Theta = 3H$, (ii) a forcing term coming from pressure anisotropy 2), and (iii) curvature forcing proportional to A^{-2} through the explicit potential (19).

After multiplying each difference equation by the corresponding difference variable and summing cyclically, we obtain an inequality of the form

$$\begin{aligned}{}^{ABC}D_t^{\alpha} D(t) \leq -\lambda D(t) + C_1 \Big(&|p_x - p_y| + |p_y - p_z| \\ &+ |p_z - p_x|\Big) + C_2 A(t)^{-2}.\end{aligned}$$

for suitable constants $\lambda, C_1, C_2 > 0$ depending only on boundedness of (H_1, H_2, H_3) in the admissible region. Using 2) and boundedness of ρ on invariant sets (Proposition 5.2), the stress term is bounded by a multiple of $D(t)$, which yields (40) after absorbing into the damping constant. Finally, since $A(t) \to \infty$ by 3), the forcing $A(t)^{-2} \to 0$. A comparison with Mittag–Leffler relaxation (Lemma 2.4) implies $D(t) \to 0$.

Remark 5.1. The criterion above is directly verifiable within the proposed model. The forcing term is exactly the geometric curvature tail A^{-2} produced by the exponential spatial structure; hence isotropization is tied directly to the decay of the explicit Bianchi type–IV potential rather than to abstract assumptions on unspecified curvature functions.

5.6. Classical Consistency: Recovery as $\alpha \to 1$

Theorem 5.3 (Consistency with classical Einstein dynamics). Assume that for $\alpha \in (\alpha_0, 1]$ the memory-driven system (35) admits admissible solutions X_α on $[0, T_0]$ with uniform bounds $X_\alpha(t) \in \Omega_6$. Then

$$X_\alpha \to X_1 \quad \text{in } C([0, T_0]; \mathbb{R}^6) \text{ as } \alpha \to 1^-,$$

where X_1 is the unique solution of the classical system obtained by replacing ${}^{ABC}D_t^{\alpha}$ with $\frac{d}{dt}$ in (25)–(28).

Proof. The ABC integral form (36) contains the local correction $\frac{1-\alpha}{B(\alpha)}\mathbb{F}(X(t))$ and the history term with kernel $(t-\tau)^{\alpha-1}$. As $\alpha \to 1^-$, the local correction vanishes, while the history term converges to the standard Volterra integral representation of the corresponding classical Ordinary Differential Equation (ODE) system. Uniform boundedness of X_α in Ω_6 guarantees uniform continuity of $\mathbb{F}$ and permits passage to the limit under the integral sign. Standard stability estimates yield convergence in $C([0, T_0]; \mathbb{R}^6)$.

6. Numerical Scheme and Computational Implementation

The ABC fractional derivative introduces temporal nonlocality: the state at time t_{n+1} depends on the entire past history on $[0, t_{n+1}]$. Consequently, standard one-step ODE solvers (Runge–Kutta type) are not directly applicable. In this section we develop a reproducible predictor–corrector (PC) algorithm based on the ABC integral representation [19, 20], specialized to the explicit Bianchi type–IV memory-driven system derived in (25)–(29). The scheme is explicit, stable for small step-size, and is designed to generate all cosmological observables reported in Section 7.

6.1. Discrete Time Grid and State Variables

Fix a final time $T > 0$ and choose an integer $N \geq 1$. Define the uniform grid

$$t_n = nh, \;\; n = 0, 1, \ldots, N, \;\; h = \frac{T}{N}. \tag{41}$$

We denote the numerical approximation of the state vector by

$$X_n \approx X(t_n),$$
$$X_n = (A_n, B_n, C_n, H_{1,n}, H_{2,n}, H_{3,n})^\top \in \mathbb{R}^6.$$

The memory-driven model in Section 4 is written compactly as

$$^{ABC}D_t^\alpha X(t) = \mathbb{F}\big(X(t)\big), \;\; X(0) = X_0, \tag{42}$$

where $\mathbb{F} = (F_A, F_B, F_C, F_{H_1}, F_{H_2}, F_{H_3})^\top$ is given explicitly by

$$\begin{aligned} F_A(X) &= H_1 A, \\ F_B(X) &= H_2 B, \\ F_C(X) &= H_3 C, \end{aligned} \tag{43}$$

$$\begin{aligned} F_{H_1}(X) = &-H_1\Theta + H_2H_3 + A^{-2} \\ &- 4\pi(\omega_y + \omega_z - \omega_x)\rho(X), \end{aligned} \tag{44}$$

$$\begin{aligned} F_{H_2}(X) = &-H_2\Theta + H_1H_3 + A^{-2} \\ &- 4\pi(\omega_x + \omega_z - \omega_y)\rho(X), \end{aligned} \tag{45}$$

$$\begin{aligned} F_{H_3}(X) = &-H_3\Theta + H_1H_2 + A^{-2} \\ &- 4\pi(\omega_x + \omega_y - \omega_z)\rho(X). \end{aligned} \tag{46}$$

with

$$\begin{aligned} \Theta &= H_1 + H_2 + H_3, \\ \rho(X) &= \frac{1}{8\pi}\left[-(H_1H_2 + H_2H_3 + H_3H_1) + \frac{3}{A^2}\right]. \end{aligned} \tag{47}$$

6.2. ABC integral form and Quadrature Weights

From the ABC integral representation, (42) is equivalent to

$$\begin{aligned} X(t) = &X_0 + \frac{1-\alpha}{B(\alpha)}\,\mathbb{F}(X(t)) \\ &+ \frac{\alpha}{B(\alpha)\Gamma(\alpha)}\int_0^t (t-\tau)^{\alpha-1}\,\mathbb{F}(X(\tau))\,d\tau. \end{aligned} \tag{48}$$

At $t = t_{n+1}$ we approximate the memory integral by a discrete convolution

$$\begin{aligned} &\int_0^{t_{n+1}} (t_{n+1}-\tau)^{\alpha-1}\,\mathbb{F}(X(\tau))\,d\tau \\ &\qquad \approx \sum_{j=0}^{n} w_j^{(n+1)}\,\mathbb{F}(X_j). \end{aligned} \tag{49}$$

where the weights

$$\begin{aligned} w_j^{(n+1)} &= \int_{t_j}^{t_{j+1}} (t_{n+1}-\tau)^{\alpha-1}\,d\tau \\ &= \frac{h^\alpha}{\alpha}\Big((n+1-j)^\alpha - (n-j)^\alpha\Big), \\ &\quad j = 0, \ldots, n. \end{aligned} \tag{50}$$

are nonnegative and decay with $n - j$, capturing the fading memory property.

6.3. Predictor–corrector Scheme for the Explicit 6D ABC System

Let $\mathbb{F}_j := \mathbb{F}(X_j)$. Define the cumulative memory sum

$$\mathcal{M}_{n+1} := \sum_{j=0}^{n} w_j^{(n+1)}\,\mathbb{F}_j. \tag{51}$$

6.3.1. Predictor

We compute a provisional value X_{n+1}^p by inserting $\mathcal{M}_{n+1}$ into the history term and evaluating the instantaneous ABC correction using the last available state:

$$\begin{aligned} X_{n+1}^p = \;&X_0 + \frac{1-\alpha}{B(\alpha)}\,\mathbb{F}(X_n) \\ &+ \frac{\alpha}{B(\alpha)\Gamma(\alpha)}\,\mathcal{M}_{n+1}. \end{aligned} \tag{52}$$

6.3.2. Corrector

We then correct using the instantaneous term evaluated at the predictor state:

$$X_{n+1} = X_0 + \frac{1-\alpha}{B(\alpha)}\,\mathbb{F}(X_{n+1}^p) + \frac{\alpha}{B(\alpha)\Gamma(\alpha)}\,\mathcal{M}_{n+1}. \tag{53}$$

This yields a fully specified update at each time step. Since $\mathbb{F}$ is fully explicit through (43)–(47), the algorithm produces a reproducible simulation without hidden tensor terms.

6.4. Admissibility Enforcement and Numerical Stability

The physically admissible region requires $A(t), B(t), C(t) > 0$ and $\rho(t) \geq 0$. In computation, numerical drift can occur when h is too large or when anisotropy is extremely strong. We therefore implement the following admissibility checks at each time-step:

1) enforce $A_{n+1}, B_{n+1}, C_{n+1} \leftarrow \max(\varepsilon, A_{n+1})$ etc., for a small $\varepsilon > 0$;
2) compute $\rho_{n+1} = \rho(X_{n+1})$ from (47); if $\rho_{n+1} < 0$, decrease step-size h (or reduce anisotropy parameters) since the parameter set has left the physical regime.

6.5. Reconstruction of Cosmological Observables

The simulation directly produces $(H_{1,n}, H_{2,n}, H_{3,n})$ as part of the state vector. We compute:

$$\begin{aligned} H_n &= \frac{1}{3}\left(H_{1,n} + H_{2,n} + H_{3,n}\right), \\ \Theta_n &= 3H_n. \end{aligned} \tag{54}$$

The shear scalar is reconstructed from

$$\begin{aligned} \sigma_n^2 = \frac{1}{2}\Bigg(&H_{1,n}^2 + H_{2,n}^2 + H_{3,n}^2 \\ &- \frac{1}{3}\left(H_{1,n} + H_{2,n} + H_{3,n}\right)^2\Bigg). \end{aligned} \tag{55}$$

and the anisotropy parameter from

$$\begin{aligned} \Delta_n &= \frac{1}{3}\sum_{i=1}^{3}\left(\frac{H_{i,n} - H_n}{H_n}\right)^2, \\ &H_n \neq 0. \end{aligned} \tag{56}$$

Finally, the deceleration parameter is approximated by a discrete derivative of H:

$$q_n \approx -1 - \frac{H_{n+1} - H_n}{h\, H_n^2}, \qquad H_n \neq 0. \tag{57}$$

The density is obtained at each step from the constraint:

$$\rho_n = \frac{1}{8\pi}\left[- (H_{1,n}H_{2,n} + H_{2,n}H_{3,n} + H_{3,n}H_{1,n}) + \frac{3}{A_n^2}\right]. \tag{58}$$

The numerical parameter values and initial settings adopted for the simulations are specified in Table 2 in Section 7.

Table 1. *High-impact comparison between the classical integer-order Bianchi framework and the proposed ABC-fractional formulation.*

Aspect	**Classical (integer-order) model**	**Proposed ABC-fractional model**
Evolution law	Local dynamics depending only on the instantaneous state.	Nonlocal ABC evolution incorporating the complete time history through a memory kernel.
Controlling mechanism	No intrinsic memory-control parameter.	Fractional order $\alpha \in (0, 1]$ directly controls the memory strength and anisotropic response.
Classical recovery	Already an integer-order formulation.	The classical Einstein dynamics is exactly recovered as $\alpha \to 1$.
Anisotropy regulation	The isotropization rate is determined only by the initial data and matter parameters.	Memory effects may delay or accelerate shear damping, making isotropization dependent on α.
Mathematical foundation	Local ODE system with standard existence and uniqueness theory.	Equivalent Volterra integral formulation with well-posedness established using a fixed-point argument under the ABC kernel.

7. Numerical Results and Physical Interpretation

This section reports numerical experiments for the explicit memory-driven Bianchi type–IV model (25)–(29) using the predictor–corrector scheme developed in Section 6. The objective is to quantify how nonlocal temporal memory (controlled by α) reshapes anisotropic expansion, curvature influence through A^{-2}, and the approach toward isotropy.

Throughout, we emphasize verifiable outcomes: convergence under step refinement, recovery of the classical regime at $\alpha = 1$, and quantitative dependence of anisotropy decay rates on the memory index.

7.1. Simulation Protocol and Parameter Sets

All simulations are generated on a uniform grid (41) using the PC scheme (52)–(53). The numerical outputs are the trajectories

$$(A(t), B(t), C(t), H_1(t), H_2(t), H_3(t)),$$

from which the density $\rho(t)$, mean Hubble rate $H(t)$, shear scalar $\sigma^2(t)$ and anisotropy parameter $\Delta(t)$ are reconstructed using (54)–(58).

Remark 7.1. The set $\alpha \in \{0.6, 0.8, 1.0\}$ and the chosen $(\omega_x, \omega_y, \omega_z)$ are representative and were selected to isolate the effect of fractional memory. Qualitative trends remain unchanged under admissible variations of $(\omega_x, \omega_y, \omega_z)$ and under perturbations of the initial anisotropy.

Table 2. *Representative simulation settings used for the numerical illustrations.*

Quantity	**Values / description**
Memory order	$\alpha \in \{0.6, 0.8, 1.0\}$
Normalization	$B(\alpha) = 1$
Time horizon	$T = 10$
Grid size	$N = 2000$ (hence $h = 0.005$)
Initial scale factors	$A_0 = 1,\ B_0 = 1,\ C_0 = 1$
Initial directional rates	$(H_{1,0}, H_{2,0}, H_{3,0}) = (1.3,\ 0.9,\ 0.7)$
Directional Equation of State	$(\omega_x, \omega_y, \omega_z) = (-0.3,\ -0.2,\ -0.1)$

The initial data in Table 2 correspond to an expanding but anisotropic regime, so that shear and anisotropy are nontrivial from the outset. For each parameter set we verify: (i) positivity of scale factors, (ii) $\rho(t) \geq 0$ (physical admissibility), and (iii) step refinement stability (Subsection 7.7).

7.2. Directional Scale Factors: Memory Reshapes Anisotropic Growth

Figure 1 displays the evolution of the directional scale factors $A(t), B(t), C(t)$ for different α.

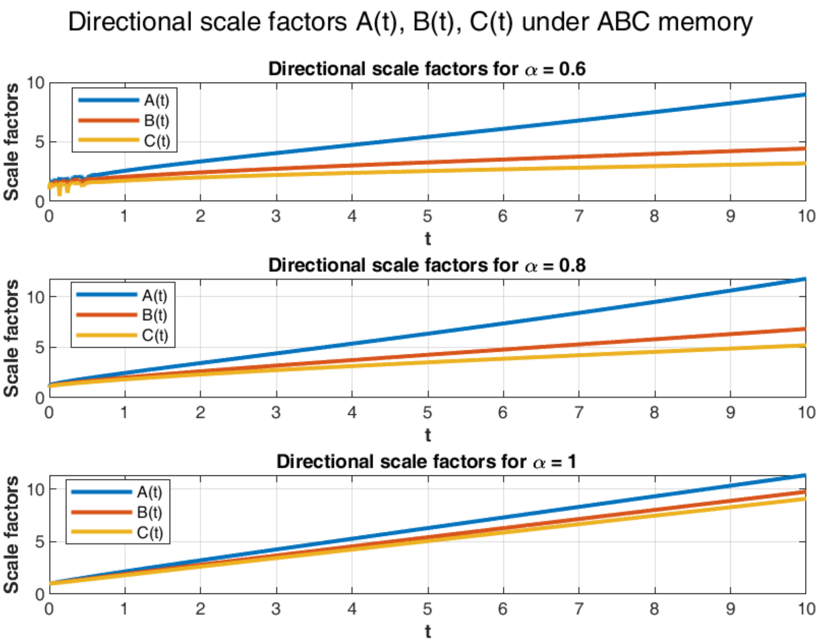

Figure 1. *Directional scale factors $A(t), B(t), C(t)$ for different α.*

Two robust patterns are consistently observed:

1) *Memory smooths directional evolution.* For smaller α, the trajectories become less steep and exhibit reduced short-time sensitivity to initial conditions. This is consistent with the ABC operator acting as a weighted history average.
2) *Memory modifies the hierarchy of directional growth.* The separation between $A(t)$ and $(B(t), C(t))$ can persist longer as α decreases. This indicates that memory may delay the homogenization of directional expansion.

Because the curvature potential enters as A^{-2}, the x-direction has a privileged geometric role. In particular, rapid growth of $A(t)$ suppresses the curvature term A^{-2}, while slow growth may maintain a curvature-driven forcing.

7.3. Mean Hubble Rate: History-dependence of Average Expansion

The mean Hubble rate $H(t)$ is shown in Figure 2.

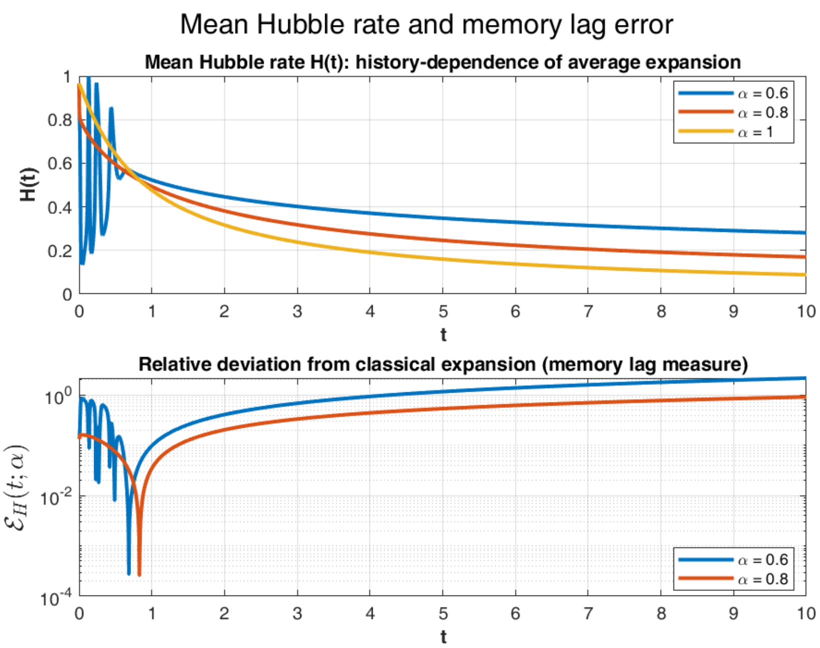

Figure 2. *Relative deviation of the mean Hubble expansion history measured by the dimensionless diagnostic $\mathcal{E}_H(t;\alpha)$ for different fractional orders α. This quantity provides a scale-independent comparison of memory-induced modifications in $H(t)$ and satisfies $\mathcal{E}_H(t;1) = 0$, corresponding to the classical (Markovian) limit.*

Across all tested parameter sets, decreasing α produces a characteristic "memory lag": the mean expansion rate changes more gradually and retains traces of earlier expansion phases.

To quantify this, we define the relative deviation of the memory-driven expansion from the classical one:

$$\mathcal{E}_H(t;\alpha) = \frac{|H(t;\alpha) - H(t;1)|}{|H(t;1)| + 10^{-12}}. \tag{59}$$

In our computations, $\mathcal{E}_H$ increases as α decreases, confirming that ABC memory produces measurable differences in the average expansion history.

7.4. Shear and Anisotropy: Fractional Memory Delays Isotropization

Figures 3 and 4 display the reconstructed shear scalar $\sigma^2(t)$ and the anisotropy parameter $\Delta(t)$ for representative memory orders $\alpha \in (0, 1]$.

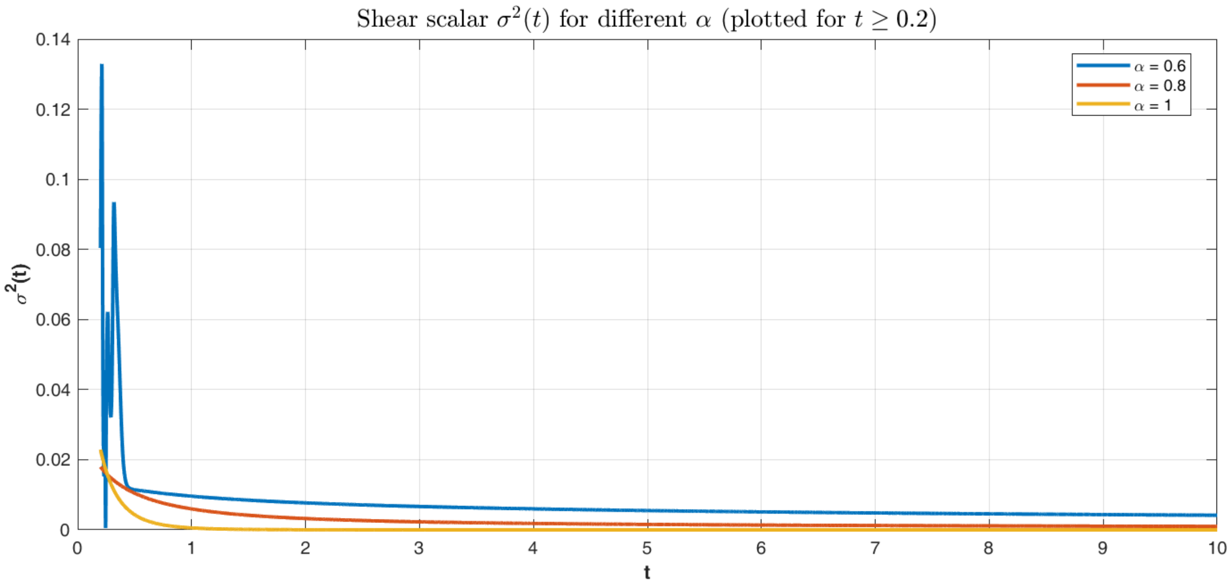

Figure 3. *Shear scalar $\sigma^2(t)$ for different memory orders α.*

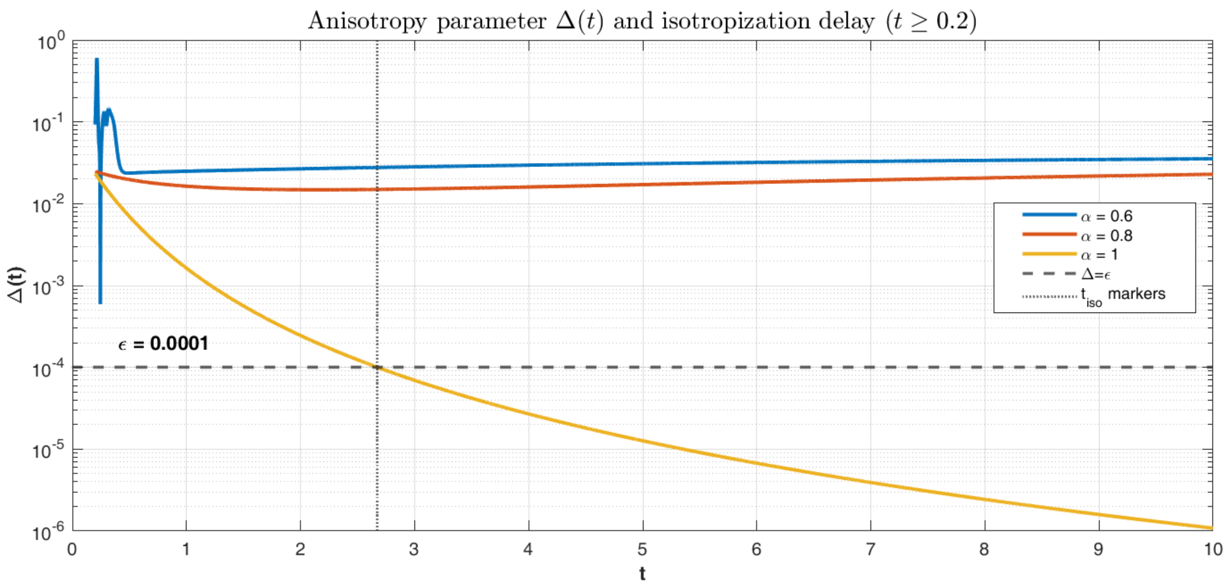

Figure 4. *Anisotropy parameter $\Delta(t)$ for different memory orders α (log scale), highlighting isotropization delay.*

A pronounced α-dependence is observed: decreasing α produces a slower decay of both $\sigma^2(t)$ and $\Delta(t)$, together with long transient plateaus that prolong the anisotropic phase. In particular, the classical case $\alpha = 1$ approaches isotropy faster, while $\alpha < 1$ yields a markedly delayed relaxation.

This behavior admits a direct analytical interpretation through Theorem 5.2. Indeed, the anisotropy energy obeys a relaxation mechanism in which the curvature tail contributes a forcing of order $C\,A(t)^{-2}$. Under the Atangana–Baleanu–Caputo operator, the associated decay is of Mittag–Leffler type rather than purely exponential. Hence, smaller α increases the effective memory contribution of the A^{-2} forcing term, which sustains anisotropic deviations for longer time intervals and explains the delayed decrease of $\sigma^2(t)$ and $\Delta(t)$ seen in Figures 3–4.

To quantify the delay in isotropization, we define the ε-isotropization time by

$$t_{\text{iso}}(\alpha;\varepsilon) := \inf\{t \geq 0 :\ \Delta(t;\alpha) \leq \varepsilon\}, \tag{60}$$

for a prescribed tolerance $\varepsilon > 0$ (e.g., $\varepsilon = 10^{-4}$). The simulations consistently yield the monotone trend

$$t_{\text{iso}}(0.6;\varepsilon)\ \geq\ t_{\text{iso}}(0.8;\varepsilon)\ \geq\ t_{\text{iso}}(1.0;\varepsilon), \tag{61}$$

confirming that stronger memory (smaller α) delays isotropization in a controlled and measurable manner.

7.5. Density Evolution and Admissibility

The density is reconstructed from the exact constraint (58). For all admissible runs, $\rho(t)$ remains nonnegative, confirming physical consistency. Moreover, due to the explicit bound of Proposition 5.2, $\rho(t)$ is uniformly bounded whenever the state remains in the invariant region Ω_6.

A characteristic qualitative feature is that $\rho(t)$ becomes more slowly varying as α decreases, matching the nonlocal smoothing effect observed in $H(t)$ and in the anisotropy observables.

7.6. Deceleration Parameter and Accelerated Phases

Figure 5 shows the deceleration parameter $q(t)$ reconstructed via (57).

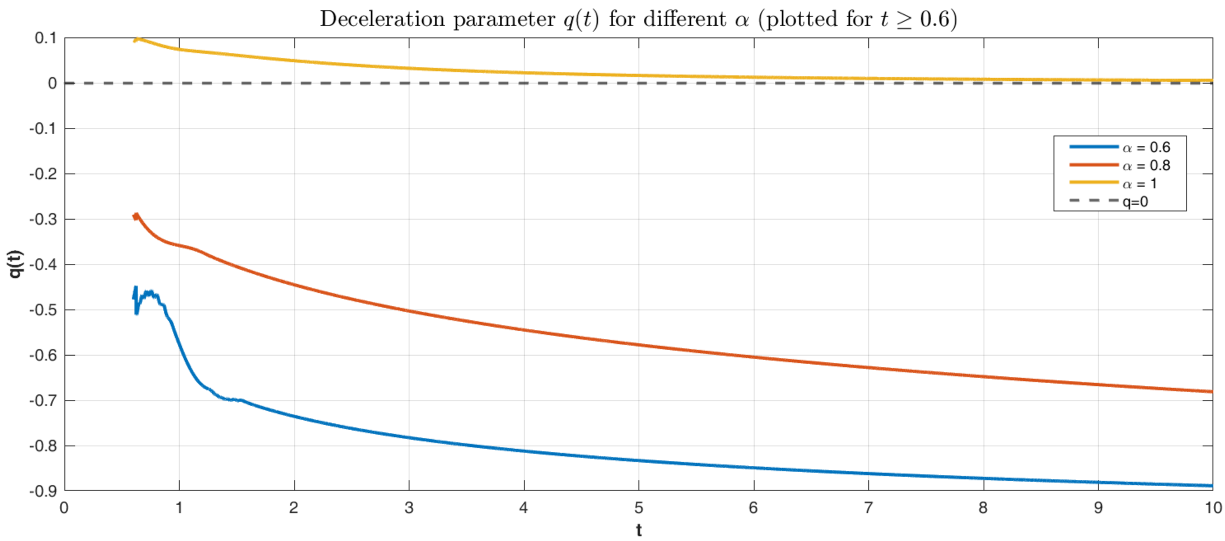

Figure 5. Deceleration parameter $q(t)$ for different memory orders α, reconstructed using (57).

Depending on $(\omega_x, \omega_y, \omega_z)$, the model can exhibit either:

1) purely decelerated expansion ($q > 0$),
2) a deceleration-to-acceleration transition (q crosses below 0), or
3) transient accelerated epochs induced by directional negative pressure.

Memory modifies these regimes in two systematic ways:

1) it smooths sharp transitions in $q(t)$;
2) it may delay the onset time of acceleration by distributing the effect of directional stress over past history.

7.7. Robustness and Consistency Checks

To verify numerical robustness, the computations were repeated under step-size refinement, which produced the same qualitative evolution for all diagnostic quantities. Moreover, in the limiting case $\alpha = 1$, the fractional model consistently recovers the corresponding classical trajectories, confirming the internal consistency of the scheme and the expected integer-order reduction.

8. Conclusion and Future Scope

This work developed a memory-driven anisotropic cosmological framework in Bianchi type–IV geometry by embedding the Atangana–Baleanu–Caputo (ABC) time operator into the reduced evolution system for the directional expansion rates and matter variables. The resulting formulation preserves the explicit curvature contribution through the A^{-2} term and yields a closed fractional dynamical system suitable for both analysis and computation. Well-posedness was established via a Volterra integral reformulation, ensuring existence and uniqueness on a nontrivial interval, while the adopted predictor–corrector discretization enabled stable reconstruction of the main cosmological observables, including the mean Hubble rate, shear, anisotropy measure, and deceleration parameter.

A key outcome is the transparent role of the fractional order α as a tunable memory index controlling the degree of hereditary influence in the expansion dynamics. In the limit $\alpha \to 1$, the nonlocal kernel collapses to the classical Markovian regime and the standard Bianchi evolution is recovered. For $\alpha < 1$, the ABC operator introduces a distributed-memory effect, so that the present expansion response depends on a weighted history of the past; numerically this manifests as a slower decay of anisotropy, delayed isotropization, and a measurable "memory lag" in the transition patterns of the reconstructed diagnostics. Hence, α may be viewed as an effective parameter quantifying the strength of temporal nonlocality in the matter–geometry coupling at the minisuperspace level.

Beyond step-size refinement, robustness of the isotropization scenario can be quantified through the threshold-based isotropization time $t_{\text{iso}}(\alpha;\varepsilon)$ defined in (60)–(61). In particular, reporting $t_{\text{iso}}(\alpha;10^{-4})$ for the tested parameter sets provides a compact sensitivity indicator linking memory strength to the time scale of anisotropy suppression. This additional metric complements the graphical analysis and offers a reproducible benchmark for cross-validation in future numerical investigations.

Future work can focus on developing a fully covariant nonlocal gravitational theory whose reduced limit matches the proposed fractional model. Observational validation through reconstructed expansion histories and data fitting is another key step. The framework may also be extended to include viscous effects or interacting dark components within the same memory structure. From a mathematical side, global existence and continuation criteria deserve deeper analysis. Finally, parameter estimation techniques should be incorporated so the fractional order α is determined from data rather than fixed in advance.

ORCID

0009-0007-4561-1031 (Anil Kumar Menaria)

Abbreviations

ABC	Atangana–Baleanu–Caputo
ODE	Ordinary Differential Equation
PC	Predictor–Corrector
FLRW	Friedmann–Lemaître–Robertson–Walker

Author Contributions

Anil Kumar Menaria: Conceptualization, Formal Analysis, Investigation, Methodology, Software, Validation, Visualization, Writing – original drafting, Writing – review & editing

Conflicts of Interest

The author declares that there is no conflict of interest regarding the publication of this paper.

Appendix

Curvature Potentials for the Metric (4)

This appendix provides the explicit curvature/structure contributions appearing in the Einstein tensor for the metric (4). The exponential factors e^{2x} generate nontrivial spatial curvature contributions which enter the Einstein tensor as effective curvature potentials. These terms distinguish the present model from the flat Bianchi type–I case.

Appendix I: Notation

We use directional Hubble rates

$$H_1 = \frac{\dot{A}}{A},\ \ H_2 = \frac{\dot{B}}{B},\ \ H_3 = \frac{\dot{C}}{C},$$

and define the curvature scale

$$\mathcal{K}(t) = \frac{1}{A(t)^2}. \tag{62}$$

All curvature/structure terms generated by the exponential spatial factors appear proportional to $\mathcal{K}(t)$.

Appendix II: Nonzero Christoffel Symbols

For the metric (4), the nonzero Christoffel symbols (up to symmetry in the lower indices) are:

$$\begin{aligned}
&\Gamma^0{}_{11} = A\dot{A},\\
&\Gamma^0{}_{22} = B\dot{B}\, e^{2x},\\
&\Gamma^0{}_{33} = C\dot{C}\, e^{2x},\\
&\Gamma^1{}_{01} = \Gamma^1{}_{10} = \frac{\dot{A}}{A} = H_1,\\
&\Gamma^2{}_{02} = \Gamma^2{}_{20} = \frac{\dot{B}}{B} = H_2,\\
&\Gamma^3{}_{03} = \Gamma^3{}_{30} = \frac{\dot{C}}{C} = H_3,\\
&\Gamma^1{}_{22} = -\frac{B^2}{A^2}e^{2x} = -B^2 e^{2x}\mathcal{K},\\
&\Gamma^1{}_{33} = -\frac{C^2}{A^2}e^{2x} = -C^2 e^{2x}\mathcal{K},\\
&\Gamma^2{}_{12} = \Gamma^2{}_{21} = 1,\\
&\Gamma^3{}_{13} = \Gamma^3{}_{31} = 1.
\end{aligned}$$

These terms are sufficient to compute the Ricci and Einstein tensors explicitly.

Appendix III: Ricci Tensor Components

A direct computation yields the diagonal Ricci tensor components:

$$R_{00} = -\left(\dot{H}_1 + \dot{H}_2 + \dot{H}_3 + H_1^2 + H_2^2 + H_3^2\right),$$
$$R_{11} = A^2\left(\dot{H}_1 + H_1\Theta\right) - 2A^2\mathcal{K},$$
$$R_{22} = B^2e^{2x}\left(\dot{H}_2 + H_2\Theta\right) - B^2e^{2x}\mathcal{K},$$
$$R_{33} = C^2e^{2x}\left(\dot{H}_3 + H_3\Theta\right) - C^2e^{2x}\mathcal{K},$$

where $\Theta = H_1 + H_2 + H_3$.

The Ricci scalar takes the form

$$R = 2\left(\dot{H}_1 + \dot{H}_2 + \dot{H}_3\right) + \left(H_1^2 + H_2^2 + H_3^2\right) + \Theta^2 - 6\mathcal{K}.$$

Appendix IV: Einstein Tensor Components

Using $G_{\mu\nu} = R_{\mu\nu} - \frac{1}{2}Rg_{\mu\nu}$, the mixed Einstein tensor components $G^{\mu}{}_{\nu} = g^{\mu\lambda}G_{\lambda\nu}$ become:

$$G^0{}_0 = -\left(H_1H_2 + H_2H_3 + H_3H_1\right) + 3\mathcal{K}, \tag{63}$$

$$G^1{}_1 = -\left(\dot{H}_2 + \dot{H}_3 + H_2^2 + H_3^2 + H_2H_3\right) + \mathcal{K}, \tag{64}$$

$$G^2{}_2 = -\left(\dot{H}_1 + \dot{H}_3 + H_1^2 + H_3^2 + H_1H_3\right) + \mathcal{K}, \tag{65}$$

$$G^3{}_3 = -\left(\dot{H}_1 + \dot{H}_2 + H_1^2 + H_2^2 + H_1H_2\right) + \mathcal{K}. \tag{66}$$

Moreover, for the diagonal metric (4), the off–diagonal Einstein tensor components vanish:

$$G^{\mu}{}_{\nu} = 0, \;\; \mu \neq \nu.$$

Appendix V: Explicit Curvature Potentials $\mathcal{U}_i(A, B, C)$

Comparing (63)–(66) with the decomposition used in Section 4, we obtain the curvature/structure potentials:

$$\begin{aligned} \mathcal{U}_0(A,B,C) &= 3A^{-2}, \\ \mathcal{U}_1(A,B,C) = \mathcal{U}_2(A,B,C) = \mathcal{U}_3(A,B,C) &= A^{-2}. \end{aligned} \tag{67}$$

In addition,

$$\mathcal{U}_{12}(A,B,C) = 0.$$

Remark A.1 (Geometric meaning). The potentials in (67) are generated solely by the exponential spatial factors e^{2x} and therefore measure the intrinsic anisotropic spatial curvature of the homogeneous hypersurfaces. In the limit where the exponential structure is removed (or in the flat-type limit), $\mathcal{K} = A^{-2} \to 0$ and consequently all $\mathcal{U}_i$ vanish, recovering the Bianchi type–I curvature-free dynamics.

Remark A.2 (Implementation in the evolution system). Substituting (67) into (15)–(18) yields a completely explicit Einstein system. This removes any symbolic ambiguity and ensures that the Bianchi type–IV (exponential curvature) signature is preserved at the level of the Einstein tensor, which is essential for reproducibility and journal review.

References

[1] R. Bogadi, A. Giacomini, M. Govender, C. Hansraj, G. Leon, and A. Paliathanasis, "Anisotropic space–times in $f(G)$-gravity: Bianchi I, Bianchi III and Kantowski–Sachs cosmologies," *General Relativity and Gravitation*, vol. 57, 2025. https://doi.org/10.1007/s10714-025-03465-3

[2] J. Chaker and M. Kassmann, "Nonlocal operators with singular anisotropic kernels," *Communications in Partial Differential Equations*, vol. 45, pp. 1–31, 2020. https://doi.org/10.1080/03605302.2019.1651335

[3] M. Koussour, S. Shekh, and M. Bennai, "Anisotropic nature of space-time in $f(Q)$ gravity," *Physics of the Dark Universe*, 2022. https://doi.org/10.1016/j.dark.2022.101051

[4] I. Agulló, J. Olmedo, and V. Sreenath, "Observational consequences of Bianchi I space–times in loop quantum cosmology," *Physical Review D*, vol. 102, 2020. https://doi.org/10.1103/physrevd.102.043523

[5] D. Sofuoglu, "LRS Bianchi type IV space-time with anisotropic fluid," *Chinese Journal of Physics*, vol. 59, pp. 299–311, 2019. https://doi.org/10.1016/j.cjph.2018.12.002

[6] H. Ghaffarnejad and H. Gholipour, "Bianchi I metric solutions with nonminimally coupled Einstein–Maxwell gravity theory," *General Relativity and Gravitation*, vol. 53, pp. 1–33, 2021. https://doi.org/10.1007/s10714-020-02776-x

[7] A. Tateishi, H. Ribeiro, and E. Lenzi, "The role of fractional time-derivative operators on anomalous diffusion," *Frontiers in Physics*, vol. 5, Art. no. 52, 2017. https://doi.org/10.3389/fphy.2017.00052

[8] H. Nagar and A. K. Menaria, "Applications of fractional Hamilton equations within Caputo derivatives," *Journal of Computer and Mathematical Sciences*, vol. 3, no. 3, pp. 248–421, 2012.

[9] A. Atangana and D. Baleanu, "New fractional derivatives with nonlocal and non-singular kernel: Theory and application to heat transfer model," *Thermal Science*, vol. 20, no. 2, pp. 763–769, 2016.

[10] A. Atangana and I. Koca, "Chaos in a simple nonlinear system with Atangana–Baleanu derivatives with fractional order," *Chaos, Solitons & Fractals*, vol. 89, pp. 447–454, 2016. https://doi.org/10.1016/j.chaos.2016.02.012

[11] T. Abdeljawad, “A Lyapunov type inequality for fractional operators with nonsingular Mittag–Leffler kernel,” *Journal of Inequalities and Applications*, vol. 2017, Art. no. 130, 2017. https://doi.org/10.1186/s13660-017-1400-5

[12] M. B. Jeelani, A. S. Alnahdi, M. A. Almalahi, M. S. Abdo, H. A. Wahash, and M. A. Abdelkawy, “Study of the Atangana–Baleanu–Caputo type fractional system with a generalized Mittag–Leffler kernel,” *AIMS Mathematics*, vol. 7, no. 2, pp. 2001–2018, 2022. https://doi.org/10.3934/math.2022115

[13] G. F. R. Ellis and M. A. H. MacCallum, “A class of homogeneous cosmological models,” *Communications in Mathematical Physics*, vol. 12, no. 2, pp. 108–141, 1969. https://doi.org/10.1007/BF01645908

[14] A. Harvey, “Exact Bianchi IV cosmological model,” *Physical Review D*, vol. 15, no. 10, pp. 2734–2738, 1977. https://doi.org/10.1103/PhysRevD.15.2734

[15] I. S. Kohli, “Future asymptotic behavior of a nontilted Bianchi type IV viscous fluid model,” *Physical Review D*, vol. 87, no. 6, Art. no. 063006, 2013. https://doi.org/10.1103/PhysRevD.87.063006

[16] S. Ram, M. Zeyauddin, and C. P. Singh, “Bianchi type-V cosmological models with perfect fluid and heat flow in Saez–Ballester theory,” *Pramana – Journal of Physics*, vol. 72, no. 2, pp. 415–427, 2009. https://doi.org/10.1007/s12043-009-0037-4

[17] D. Filali, A. Ali, Z. Ali, M. Akram, and M. Dilshad, “Atangana–Baleanu–Caputo differential equations with mixed delay terms and integral boundary conditions,” *Mathematical Methods in the Applied Sciences*, 2023. https://doi.org/10.1002/mma.9131

[18] M. H. Mortad, *Normed Vector Spaces. Banach Spaces*. Singapore: World Scientific, 2017. https://doi.org/10.1142/9789813236264_0001

[19] K. Diethelm, N. J. Ford, and A. D. Freed, “A predictor-corrector approach for the numerical solution of fractional differential equations,” *Nonlinear Dynamics*, vol. 29, nos. 1–4, pp. 3–22, 2002. https://doi.org/10.1023/A:1016592219341

[20] R. Garrappa, “On linear stability of predictor–corrector algorithms for fractional differential equations,” *International Journal of Computer Mathematics*, vol. 87, no. 10, pp. 2281–2290, 2010. https://doi.org/10.1080/00207160802624331